

The Sol-Gel Process Simulated by Cluster-Cluster Aggregation

Anwar Hasmy and Rémi Jullien

Laboratoire de Science des Matériaux Vitreux, UA 1119 CNRS, Université Montpellier II, Place

Eugène Bataillon, 34095 Montpellier Cedex 5, France

(September 17, 2018)

Abstract

The pair-correlation function $g(r, t)$ and its Fourier transform, the structure factor $S(q, t)$, are computed during the gelation process of identical spherical particles using the diffusion-limited cluster-cluster aggregation model in a box. This numerical analysis shows that the time evolution of the characteristic cluster size ξ exhibits a crossover close to the gel time t_g which depends on the volumic fraction c . In this model t_g tends to infinity when the box size L tends to infinity. For systems of finite size, it is shown numerically that, when $t < t_g$, the wave vector q_m , at which $S(q, t)$ has a maximum, decreases as $S(q_m, t)^{-1/D}$, where D is an apparent fractal dimension of clusters, as measured from the slope of $S(q, t)$. The time evolution of the mean number of particles per cluster \bar{n} is also investigated. Our numerical results are in qualitative agreement with small angle scattering experiments in several systems.

I. INTRODUCTION

In the last years, the kinetics of aggregation has been widely studied [1]. It has been studied experimentally in a large number of systems like aqueous metal colloids [2], silicon tetramethoxyde [3] and tetraethoxyde [4], alumino-silicates [5], colloidal silica [6], polystyrene [7–10], and oil in water emulsions [11,12]. Using small-angle scattering techniques it has been suggested that some of these systems [5,7–9,11,12] grow like diffusion-limited cluster-cluster aggregation (DLCA) [13–15]. Numerically, the gelation process in DLCA has been investigated by analyzing the cluster size distribution and the mean cluster size, as a function of the time t using both the Smoluchowski equation [16] and the DLCA model in 2 dimensions [17]. On the other hand, recently [18,19] it has been shown that, when the volumic fraction c , or concentration, is greater than a characteristic gel concentration c_g , DLCA model leads to a homogeneous gelling network of connected fractal clusters of mean size ξ .

In some systems [4,5,8–12] where fractal clusters grow separately until obtaining a system of connected fractal clusters at large t , the wave-vector-dependent scattering function $S(q, t)$ exhibits a maximum in the wave vector q_m -value (which is inversely proportional to ξ) at a given time t . This maximum can be interpreted as a crossover between the fractal regime (intermediate q -values where $S(q, t) \propto q^{-D}$) and the homogeneous regime (small q -values). Moreover, some very interesting relations on the $S(q)$ curve (see below equations 7) have been established on various systems [8,10]. Since scaling relations are known to be of wide applications (“universality”) it is worth studying them here. Another interesting experimental results [5] reveal that the gyration radius R_g (which is proportional to ξ) saturates close to t_g , the time where the system can be considered as a gelling network.

In this paper, we present some new results obtained from our numerical study of the gelation process using diffusion limited cluster-cluster aggregation in a box [13–15], where a sufficiently large initial concentration has been considered in order to obtain a gelling network of connected clusters at the end of the aggregation process. We have calculated numerically the mean number of particles per cluster \bar{n} and their mean size ξ as a function

of time t as well as the correlation function $g(r, t)$, and the scattering function $S(q, t)$. We show that there exists a crossover at t_g such that, for $t < t_g$, ξ increases when t increases, and for $t > t_g$, the characteristic length ξ remains constant and equal to its value obtained near t_g . The location of this crossover is pushed toward the low- t values when c increases. For $c \gg c_g$ the normalized gel time t_g/t_{tot} does not change. Additionally, the maximum of the $S(q, t)$ curve, $S(q_m, t)$, increases as $\xi^{D_{sl}}$ where D_{sl} is an apparent fractal dimension. We report on the discrepancies between the actual fractal dimension D and D_{sl} for large c -values. Finally, we discuss the qualitative agreement between our simulations and some experiments.

II. CONSTRAINTS ON THEORY

We have modeled the gelation process considering a three dimensional off-lattice extension of the original diffusion cluster-cluster aggregation model [13,14] as in ref. [19] where we have shown that such a model is well adapted to describe the aerogel structure. During the aggregation process, we can naturally define a ‘‘Monte-Carlo’’ time t_{mc} which is increased by an arbitrary constant amount δt_{mc} at each iteration. Due to the use of formula (3) of ref. [19] to choose the aggregates, the actual ‘‘physical’’ time t should be increased by the amount δt related to δt_{mc} by:

$$\delta t = \frac{\delta t_{mc}}{\sum_i n_i^\alpha} \quad (1)$$

In our calculation the time unit has been arbitrarily fixed by setting $\delta t_{mc} = 1$.

Using scaling arguments, it can be established that the whole system remains invariant if length, mass and time are conveniently rescaled simultaneously [20,21]. Changing the average mass \bar{n} by a factor b , the distance should be rescaled by $b^{1/D}$ and, using a general mean-field argument to evaluate the average time it takes for all clusters to pair up, the time should be rescaled by $b^{1-\alpha-\frac{(d-2)}{D}}$, giving:

$$n \propto t^\gamma \quad (2a)$$

with

$$\gamma = \frac{1}{1 - \alpha - \frac{d-2}{D}} \quad (2b)$$

For $\alpha = -1/D$ and $d = 3$ this reasoning gives $\gamma = 1$. In figure 1 we show the time evolution of the mean number of particles per cluster \bar{n} for three different concentrations. When $c < c_g$ \bar{n} is roughly proportional to t as expected from equation (2). However, for $c > c_g$ this dependence is only observed at short times (for $t \ll t_g$). At large times (for $t \gg t_g$) if one still assumes $\bar{n} \sim t^\gamma$, one should consider a very large exponent $\gamma \sim 4$. Note that in refs. [20,21], equation (2) was obtained under the hypothesis that the entire system remains space and time scaling invariant. This hypothesis is no longer valid when a gel is formed since the system becomes homogeneous for distances larger than ξ [18,19] and if one tries to define its global fractal dimension it should be taken as the dimension of space. Qualitatively, the observed increase of γ can be understood as a consequence of the increase of the fractal dimension. An earlier work by Gonzalez [22] suggests the same conclusion. In his paper it is shown that when D increases from 1.87 to 2.05, γ increases from 1.3 to 2.5 when using a cluster-cluster aggregation model with a sticking probability p varying from 0.5 to 0.005, reaching the chemically-limited cluster-cluster aggregation (CLCA) model [23], also called reaction-limited cluster-cluster aggregation (RLCA) [24]. An increasing γ -value with D was also found in another CLCA model also recently proposed by Gonzalez [25].

The distance that a cluster must travel before colliding with another cluster decreases when c increases so that both the gel time t_g , when it exists (i. e. for $c > c_g$), and the time at the end of the aggregation process t_{tot} should decrease as c increases. This is well observed in figure 2 where t_g and t_{tot} have been plotted as a function of c in a log-log plot. For $c < c_g$ we observe that t_{tot} is roughly inversely proportional to c while, for $c > c_g$, both t_g and t_{tot} decrease roughly as $c^{-1.75}$ (c_g is determined as explained in ref. [19]). The latter result can be simply understood if one assumes that when $c > c_g$ the scaling relation (2) holds up to $t \sim t_g$ where the system is made of clusters of mean size ξ containing ξ^D particles. The concentration being related to ξ by $c \sim \xi^{-(3-D)}$ (see ref. [19]), the relation (2) with $\gamma = 1$

gives:

$$t_g \propto c^{-\frac{D}{3-D}} \quad (3)$$

The observed exponent of -1.75 corresponds to $D \sim 1.9$ a value larger but quite close to the expected value of the fractal dimension of DLCA clusters. We point out that in our model c_g decreases as $L^{-(3-D)}$ as showed elsewhere [19], and from equation (3) one can deduce that $t_g \rightarrow \infty$ when $L \rightarrow \infty$. From figure 2 we also find that the ratio t_g/t_{tot} is almost independent on c , for $c \gg c_g$. This implies that the time taken by smaller clusters to stick to the gelling network remains a finite fraction of the total time.

The two-point correlation function $g(r, t)$ can be calculated by choosing a given path δr , and calculating the number δn of interparticle distances lying between r and $r + \delta r$, taking care of the periodic boundary conditions when investigating regions outside of the box. In order to normalize $g(r, t)$ to unity when r tends to infinity, $g(r, t)$ was defined as follows:

$$g(r, t) = \frac{\pi}{6c} \frac{1}{4\pi r^2} \frac{\delta n}{\delta r} = \frac{1}{24cr^2} \frac{\delta n}{\delta r} \quad (4)$$

The static structure factor, or scattering function, $S(q, t)$ in a system containing identical particles with mean volume fraction c is given by [26]:

$$S(q, t) = 1 + \frac{6c}{\pi} \int_0^{r_m} (g(r, t) - g_0) \frac{\sin qr}{qr} 4\pi r^2 dr \quad (5a)$$

In theory one should take $g_0 = 1$ and $r_m = \infty$. But, as explained in detail in refs. [18,19] we have calculated g_0 from the formula:

$$g_0 = \frac{\int_0^{r_m} g(r, t) 4\pi r^2 dr + \pi/6c}{\int_0^{r_m} 4\pi r^2 dr} \quad (5b)$$

which gives a g_0 value very close to one that insures that $S(q, t) \rightarrow 0$ when $q \rightarrow 0$. On the other hand, r_m was chosen equal to $\frac{L}{2}$, to avoid boundary artifacts due to the periodic boundary conditions considered in our problem.

III. RESULTS

Using equation (4), we have calculated $g(r, t)$ at all times t during the aggregation process; we have observed that all the $g(r, t)$ curves exhibit a delta peak at $r = 1$, a discontinuity at $r = 2$ and a minimum at $r = \xi$, that correspond to the typical short and long range features of DLCA aggregates [19]. In figure 3 we have plotted several $g(r, t)$ curves for $c = 0.005$ at four different t emphasizing the region near the minimum in order to show that its location (which defines the characteristic size ξ of the aggregates) is shifted to higher r -values when t increases. The function $g(r, t)$ was averaged up to 20 independent simulations, and the box size L was taken equal to 103.

Figure 4 shows ξ as function of t/t_{tot} for four different values of c . From equation (2), one expects that ξ should increase as $(t/t_{tot})^{\frac{1}{D}}$ for $t < t_g$. However, for concentrations close to c_g this power law is only verified for $t \ll t_g$. For t smaller than but close to t_g one observes a crossover regime with a smaller slope which extends down to smaller times when c is smaller. This smaller slope might be due to the interpenetration of clusters which becomes important as t approaches t_g . The cluster size ξ saturates for $t > t_g$ suggesting that, in this regime, the remaining free small clusters diffuse towards the gelling network on which they stick without changing the mean size of the large connected clusters. However, during this regime, the density of clusters increases and therefore their fractal dimension should become larger. This can be checked in figure 5 where we have plotted the fractal dimension D as a function of c . The upper curve (open squares) correspond to the "true" fractal dimension, i.e. the one estimated in real space from the power law behavior $g(r, t) \propto r^{D-3}$, for $3 < r < \xi$.

In figure 6 we show typical $S(q, t)$ curves at different times. These curves exhibit the three regimes explained elsewhere [19], damped oscillations at large q -values ($q \gg a^{-1}$), a power law $S(q, t) \propto q^{-D}$ at the intermediate q -values, and a vanishing regime for $q \ll \xi^{-1}$. In this figure we clearly see that q_m is shifted to lower q -values as t increases. This is in agreement with the results of figure 4 if one considers that q_m is proportional to ξ^{-1} (as found for $t = t_{tot}$ in ref. [19]). Additionally, it has been shown [27] that the scaled scattering

function $S(q/q_m, t)$ and the position of the peak q_m are related by:

$$S(q/q_m, t) = q_m(t)^{-\delta} F(q/q_m) \quad (6)$$

where $F(q/q_m)$ is a time-independent scaling function. In spinodal decomposition $\delta = d = 3$, while in other growth problems $\delta = D$ [8,28]. In our case, as showed in inset in figure 6, the best collapse is obtained with $\delta = 1.9$ which roughly corresponds to our previous estimate of the fractal dimension. Also, this scaling behavior can be deduced by considering that the maximum of the scattering function $S(q_m, t)$ is roughly proportional to the mean number of particles per cluster [19]:

$$S(q_m, t) \propto \xi^D \quad (7a)$$

implying:

$$q_m \propto \frac{1}{\xi} \propto S(q_m, t)^{-\frac{1}{D}} \quad (7b)$$

In figure 7 we show a log-log plot of $q_m (\approx \frac{\pi}{\xi})$ versus $S(q_m, t)$. For convenience we have reported the results for $q_m = \frac{\pi}{\xi}$ by estimating ξ from the minimum of $g(r, t)$ since in such estimation the errors are smaller than estimating q_m directly from $S(q, t)$. As expected from equation (7b) a quasi linear behavior is found for the four concentrations reported in the figure. By performing a linear regression we have estimated the exponents of (7b) which have been reported in table I together with the related fractal dimension that we call D' . In this table we have also reported the values D_{sl} obtained from the slopes of the respective $S(q, t)$ curves at the last stage of the aggregation process as well as the actual fractal dimension D obtained from $g(r, t)$. It is shown that, while D increases, D' and D_{sl} decrease when c increases, as already seen on figure 5. Similar discrepancies between D and D_{sl} were observed by Amar et al. [28] in a sub-monolayer molecular beam epitaxy model in which the aggregation regime was described by a system of connected fractal clusters. These discrepancies between D and D_{sl} might be explained by the fact that for $D > 2$ the single scattering theory considered here is not completely justified [29]. Note that, for $c > c_g$ one

has $D = 3$ for distances larger than ξ , while for $c \leq c_g$ the final system is a single fractal aggregate, with $D_{sl} = D$ as showed elsewhere [30].

IV. DISCUSSION

In this section we would like to discuss our results in comparison with several experiments. Small-angle neutron-scattering (SANS) experiments in the sol-gel process of aluminosilicates have been performed by Pouxviel et al. [5] showing that the radius of gyration R_g saturates when t approaches t_g (see figure 2 of ref. [5]). These authors have considered three different composition samples prepared under basic conditions and they obtained a fractal dimension $D \approx 1.8$ as in the DLCA case. Therefore, their results are in agreement with our numerical simulations. Another interesting study has been reported in ref. [8], where small-angle light-scattering experiments have been performed on polystyrene spheres diluted in a water-heavy-water mixture; it has been shown that $I(q_m)$ scale as q_m^z , where z is equal to -0.58 (close to the exponent reported in table I), at early stage of the growth process, and at larger t values it has been found that z becomes close to (-1/3) the typical value for spinodal decomposition. They conclude that at early stage of spinodal decomposition the growth is dominated by DLCA. Similar kind of analysis has been recently done by Hobbie et al. [10] concerning SANS experiments in a hydrogen-bonded polymer blend. But in their experiments they found $D = 2.4$ a value consistent with diffusion limited particle-cluster aggregation [31].

Other interesting results have been reported by Bibette et al. [11,12]. They have performed small angle light scattering experiments in monodisperse droplets of water emulsions in oil. They have suggested that the emulsion growth is like diffusion-limited cluster-cluster aggregation, obtaining $D \approx 1.8$. We have extracted the $I(q_m, t)$ points from their curves of figure 2 in ref. [11], that we have compared with the points obtained from our simulation when using the same c value as in the experiments ($c = 0.005$). In figure 8 we show the good agreement with the experiments, obtaining the same increasing behavior of $I(q_m, t)$ as

a function of t .

V. CONCLUSION

In conclusion, in this work we have shown that numerical simulations of DLCA model in a box can account for the growth process of several experimental systems. On the other hand, our numerical calculation of $S(q, t)$ during the DLCA process is an original investigation that extends previous numerical analysis of this growth process [1,16,17,20], leading to the theoretical explanation of additional interesting properties during the aggregation process and confirming some predictions made in some experimental studies. In particular the power law given in equation (7b) and the shape of our $S(q, t)$ curves are experimentally observed. Similar calculations with the CLCA model are in progress in order to interpret some experiments which are more likely explained by such kind of growth process.

One of us (A. H.) would like to acknowledge support from CONICIT (Venezuela).

REFERENCES

- [1] F. Family and D. P. Landau, “Kinetics of Aggregation and Gelation”, North-Holland, Amsterdam (1984).
- [2] D. A. Weitz, J. S. Huang, M. Y. Lin and J. Sung, Phys. Rev. Lett. **53**, 1657 (1984).
- [3] J. E. Martin and K. D. Keefer, Phys. Rev. A, **34**, 4988 (1986).
- [4] B. Cabane, M. Dubois and R. Duplessix, J. Physique, **48**, 2131 (1987).
- [5] J. C. Pouxviel, J. P. Boilot, A. Dauger and A. Wright, J. of Non-Cryst. Solids, **103**, 331 (1988).
- [6] F. Ferri, M. Giglio, E. Paganini and U. Perini, Europhys. Lett., f **7**, 599 (1988).
- [7] M. L. Broide and R. J. Cohen, Phys. Rev. Lett., **64**, 2026 (1990).
- [8] M. Carpineti and M. Giglio, Phys. Rev. Lett., **68**, 3327 (1992).
- [9] D. J. Robinson and J. C. Earnshaw, Phys. Rev. Lett., **71**, 715 (19 93).
- [10] E. K. Hobbie, B. J. Bauer and C. C. Han, Phys. Rev. Lett., **72**, 1830 (1994).
- [11] J. Bibette, T. G. Mason, H. Gang and D. A. Weitz, Phys. Rev. Lett., **69**, 981 (1992).
- [12] J. Bibette, T. G. Mason, H. Gang, D. A. Weitz and P. Poulin, Langmuir, **9**, 3352 (1993).
- [13] P. Meakin, Phys. Rev. Lett., **51**, 1119 (1983).
- [14] M. Kolb, R. Botet and R. Jullien, Phys. Rev. Lett., **51**, 1123 (1983).
- [15] R. Jullien and R. Botet, “Aggregation and Fractal Aggregates”, World Scientific (Singapore, 1987).
- [16] M. Thorn and M. Seesselberg, Phys. Rev. Lett., **72**, 3622 (1994).
- [17] M. Kolb and H. J. Herrmann, J. Phys. A, **18**, L435 (1985).

- [18] A. Hasmy, E. Anglaret, M. Foret, J. Pelous and R. Jullien, Phys. Rev. B, **50**, 6006 (1994).
- [19] A. Hasmy, M. Foret, E. Anglaret, J. Pelous, R. Vacher and R. Jullien, these proceedings.
- [20] R. Botet and R. Jullien, J. Phys. A., **17**, 2517 (1984).
- [21] M. Kolb, Phys. Rev. Lett., **53**, 1654 (1984).
- [22] A. E. Gonzalez, J. Phys. A, **26**, 4215 (1993)
- [23] R. Jullien and M. Kolb, J. Phys. A, **17**, L639 (1984).
- [24] W. Brown and R. Ball, J. Phys. A, **18**, L517 (1985).
- [25] A. E. Gonzalez, Phys. Rev. Lett., **71**, 2248 (1993).
- [26] L. A. Feigin and P. I. Svergun, “Structure Analysis by Small Angle X-rays and Neutron Scattering”, Academic Press (London and New York, 1967).
- [27] H. Furukawa, Adv. Phys., **34**, 703 (1985). See also K. Binder in ref. [1].
- [28] J. G. Amar, F. Family and P-M Lan, Phys. Rev. B, **50**, 8781 (1994).
- [29] M. V. Berry, J. Phys. A, **12**, 781, 1979.
- [30] H. F. van Garderen, E. Pantos, W. H. Dokter, T. P. M. Beelen, M. A. J. Michels, P. A. J. Hilbers and R. A. van Santen, preprint.
- [31] T. A. Witten and L. M. Sander, Phys. Rev. Lett., **47**, 1400 (1981).

TABLES

c	exponent ($\frac{-1}{D'}$)	D'	D_{sl}	D
0.005	-0.52	1.92	1.79	1.95
0.010	-0.54	1.85	1.77	2.02
0.015	-0.55	1.82	1.76	2.11
0.030	-0.62	1.61	1.62	2.32

TABLE I. For four concentrations considered in the simulations, we have reported the respective exponents ($\frac{-1}{D'}$) from equation (7b) and the related fractal dimensions D' , which is compared with the apparent fractal dimension D_{sl} measured from the slope of the $S(q, t)$ curve and the “true” fractal dimension D as deduced from $g(r, t)$.

FIGURES

FIG. 1. Log-log plot of \bar{n} versus ct for $L=57.7$, and for $c = 0.003$ (dashed line), $c = 0.01$ (dotted line) and $c = 0.05$ (solid line). These curves result from averages over 20 simulations.

FIG. 2. Log-log plot of t_{tot} (black symbols), and t_g (open symbols) versus c for $L=57.7$. The solid line corresponds to linear regressions and the vertical arrow show the location of c_g . These data result from averages over 20 simulations.

FIG. 3. Plot of $g(r, t)$ versus r for $L = 103$ and $c = 0.005$ at different times t of the aggregation process, $t/t_{tot}=0.027$ (dot-dashed line), $t/t_{tot}=0.01$ (dashed line), $t/t_{tot}=0.57$ (dotted line) and $t/t_{tot}=1$ (solid line). These curves result from averages over 10 simulations.

FIG. 4. Log-log plot of ξ versus t/t_{tot} for $L = 103$, and for $c = 0.005$ (open circles), $c = 0.01$ (black squares), $c = 0.015$ (open diamonds) and $c = 0.03$ (black triangles). The vertical arrows indicate the respective location of t_g . These data result from averages over 10 simulations.

FIG. 5. Log-log plot of the “true” fractal dimension D (open symbols) versus c , the open squares and open triangles correspond to $L = 57.7$ and $L = 28.85$, respectively. The black symbols denote the D_{sl} measured from the slope of the $S(q, t)$ curve for $L = 57.7$. These curves result from averages over 20 simulations.

FIG. 6. For four different times $t/t_{tot}=0.027$ (dot-dashed line), $t/t_{tot}=0.01$ (dashed line), $t/t_{tot}=0.57$ (dotted line) and $t/t_{tot}=1$ (solid line) we show the Log-log plot of $S(q, t)$ versus q . Inset: Log-log plot of $S(q/q_m, t)q_m^D$. The parameters are the same as in figure 3.

FIG. 7. Log-log plot of q_m versus $S(q_m, t)$ for $L = 103$, and for $c = 0.005$ (black circles), $c = 0.01$ (open squares), $c = 0.015$ (open diamonds) and $c = 0.03$ (black triangles). These curves result from averages over 10 simulations.

FIG. 8. Log-log plot $I(q_m, t)$ versus t_{tot} . The open symbols denote the simulation (same parameter as in figure 3), and black symbols denote experimental data from ref. [11].

fig 1

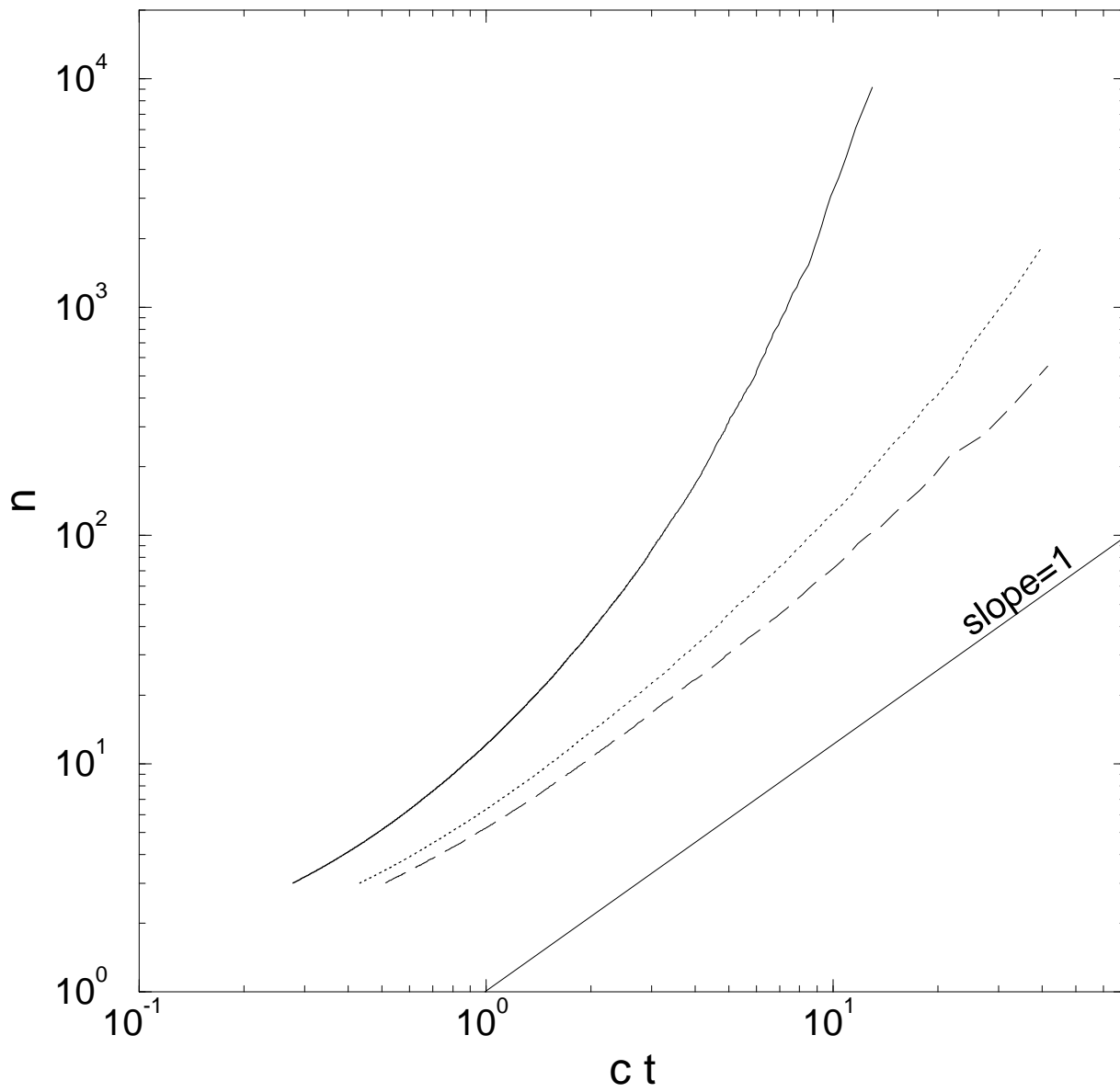


fig 2

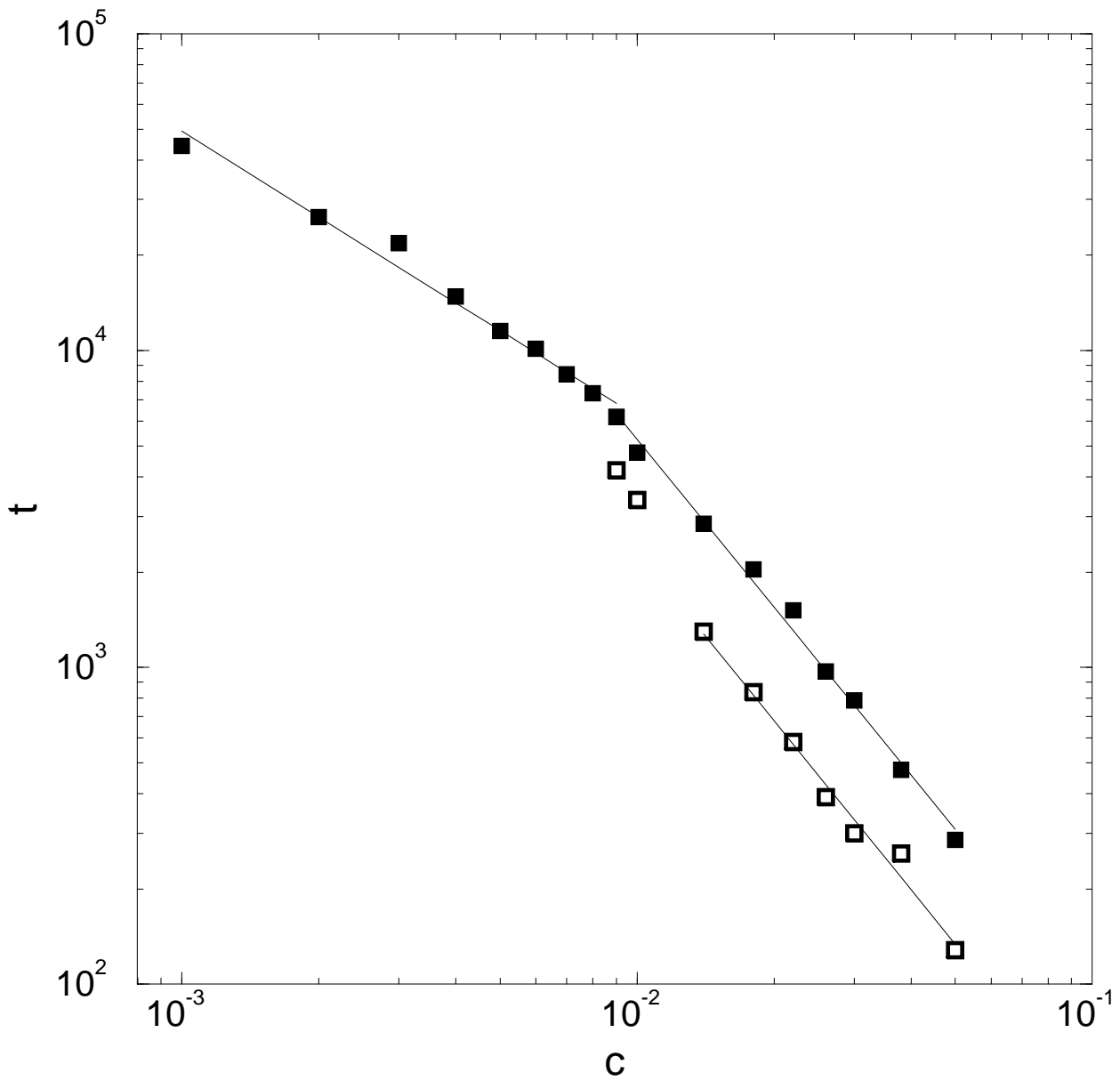


fig 3

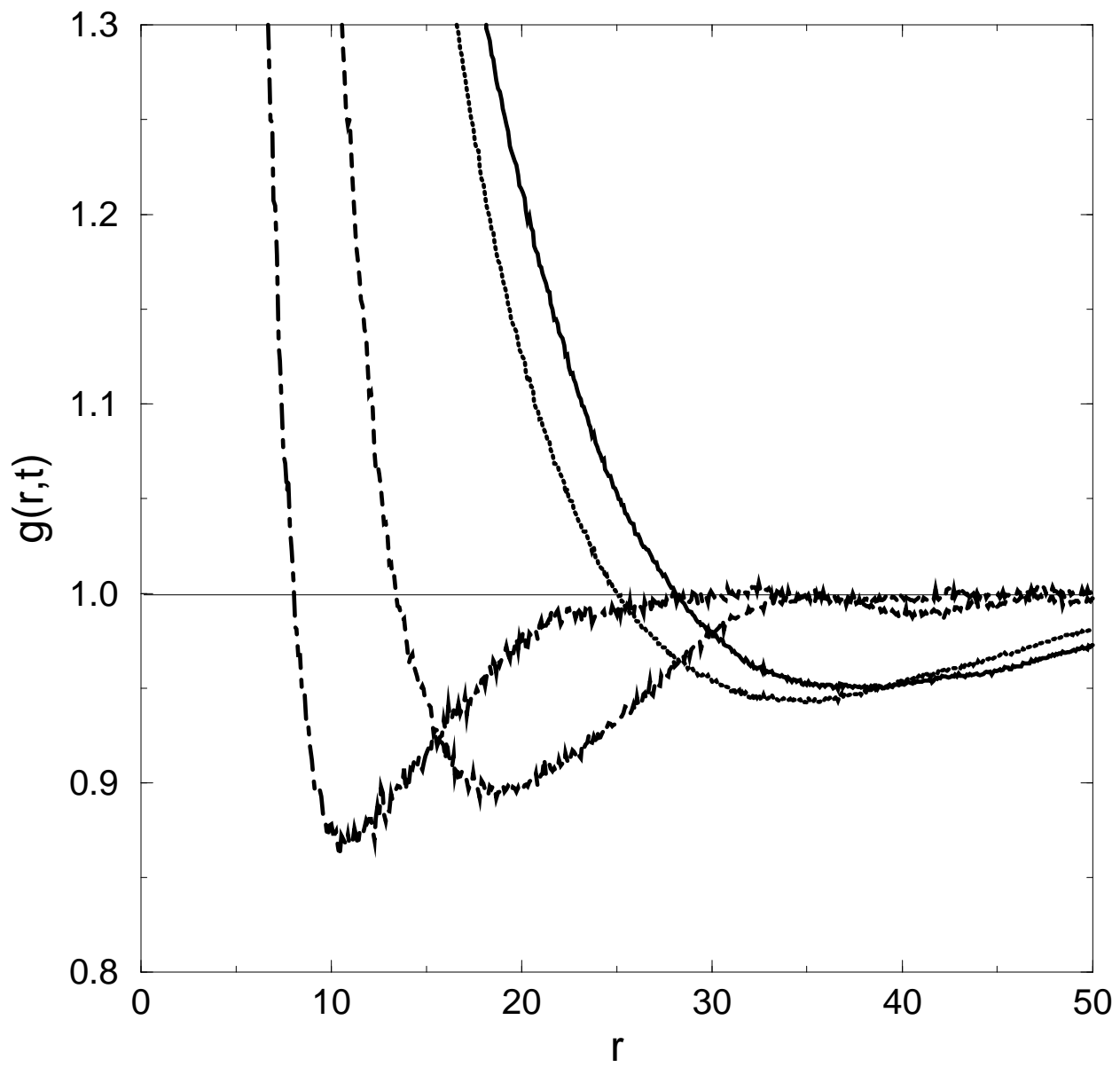


fig 4

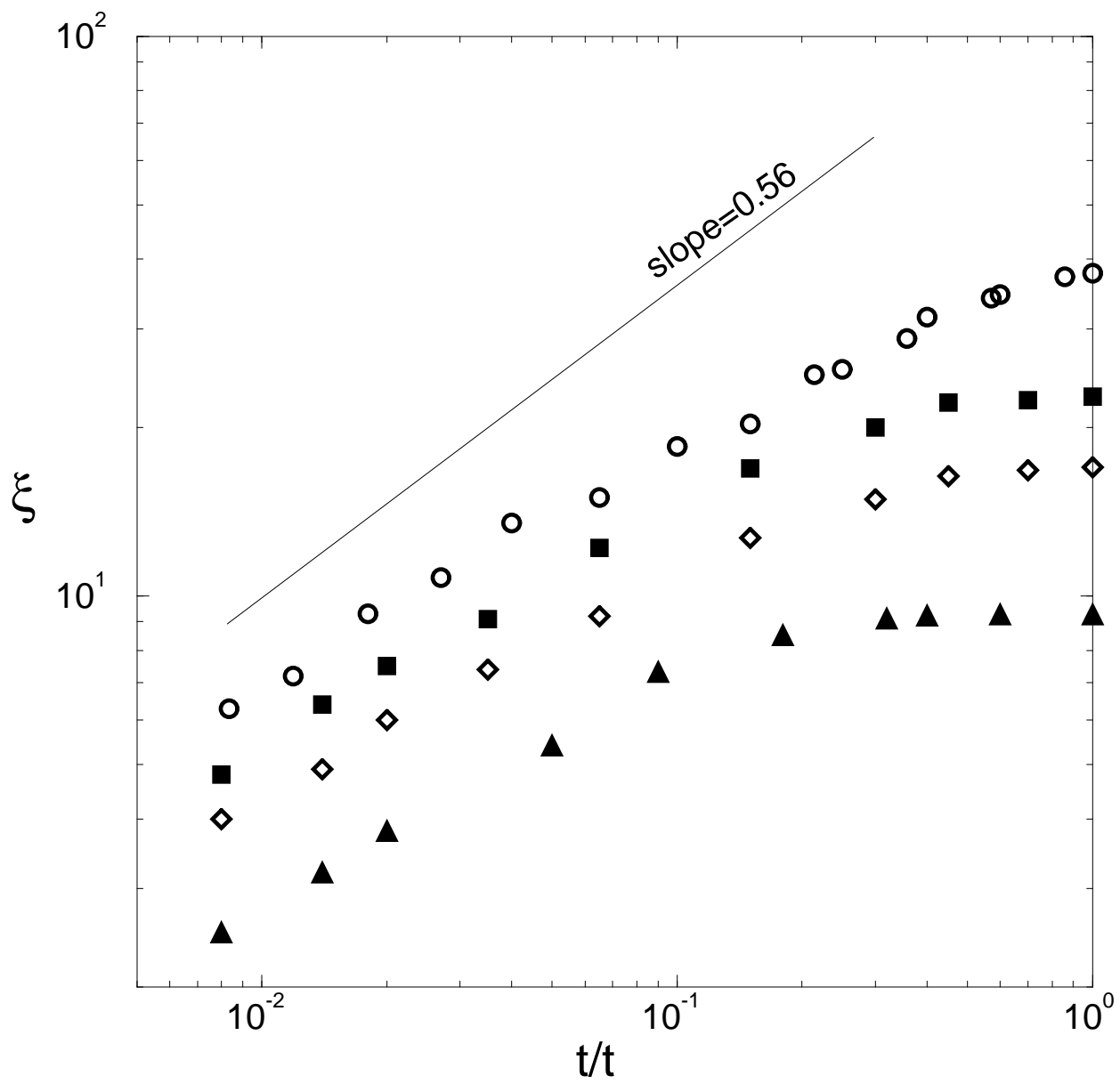


fig 5

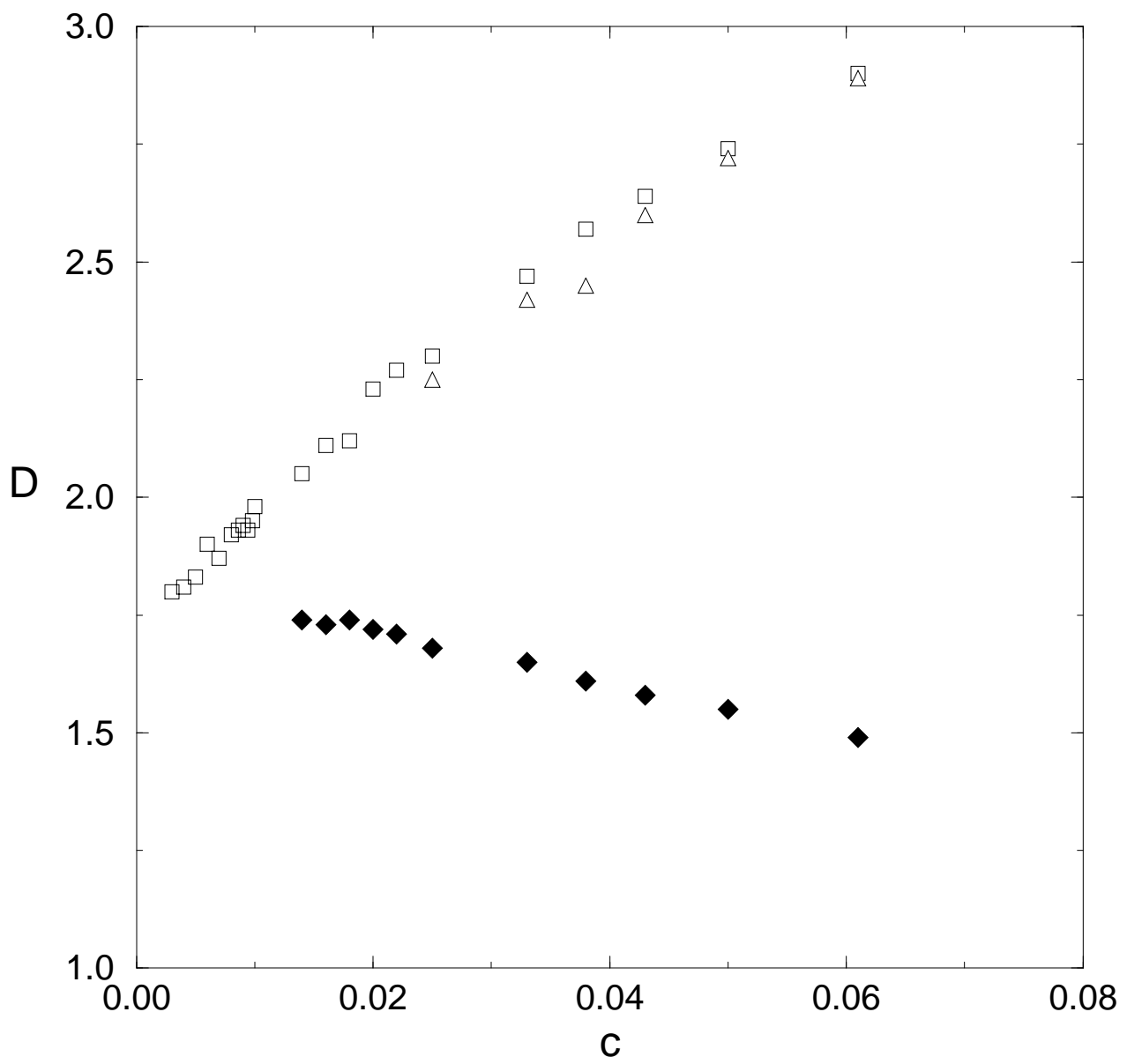


fig 6a

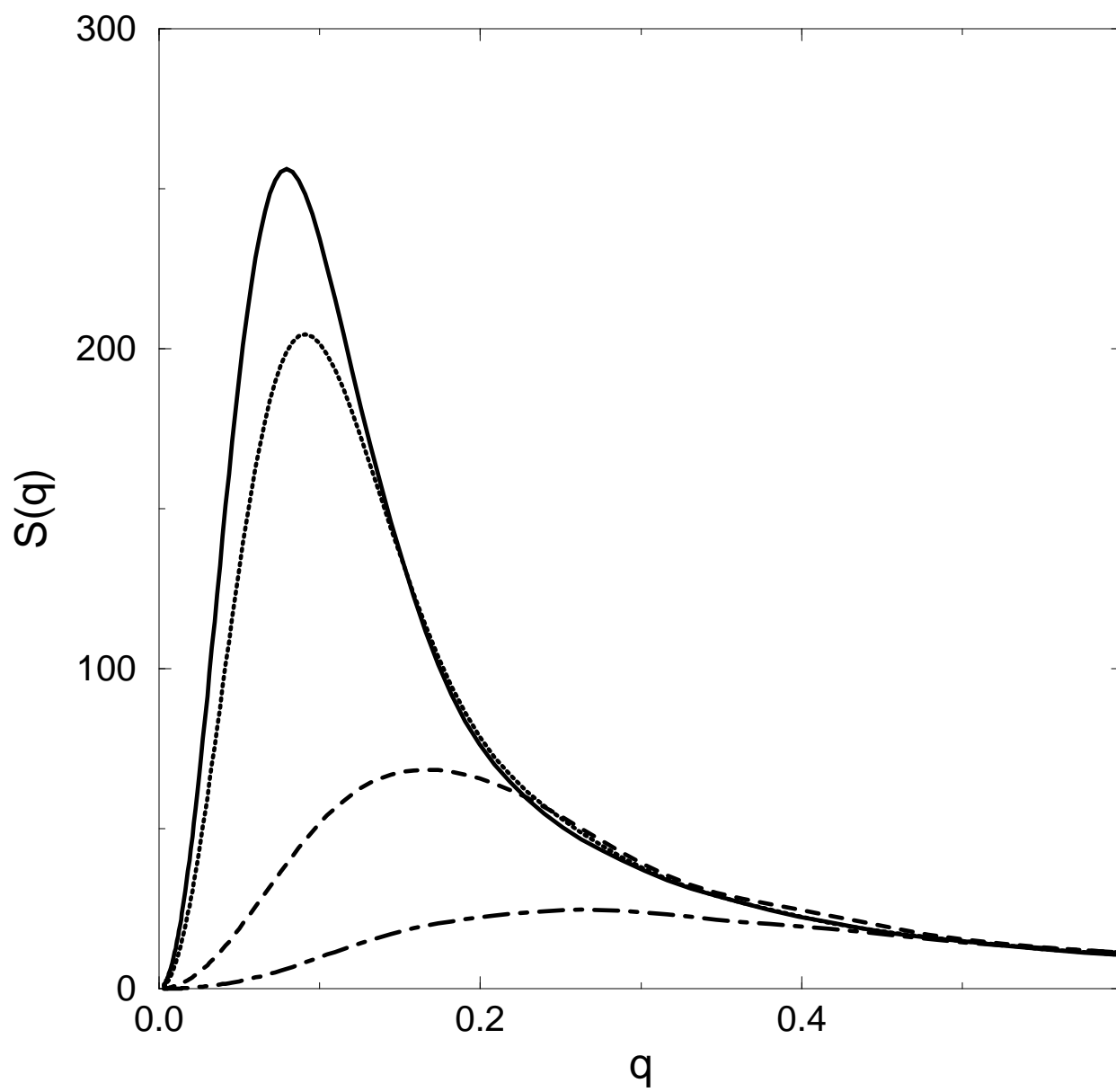


fig 6b

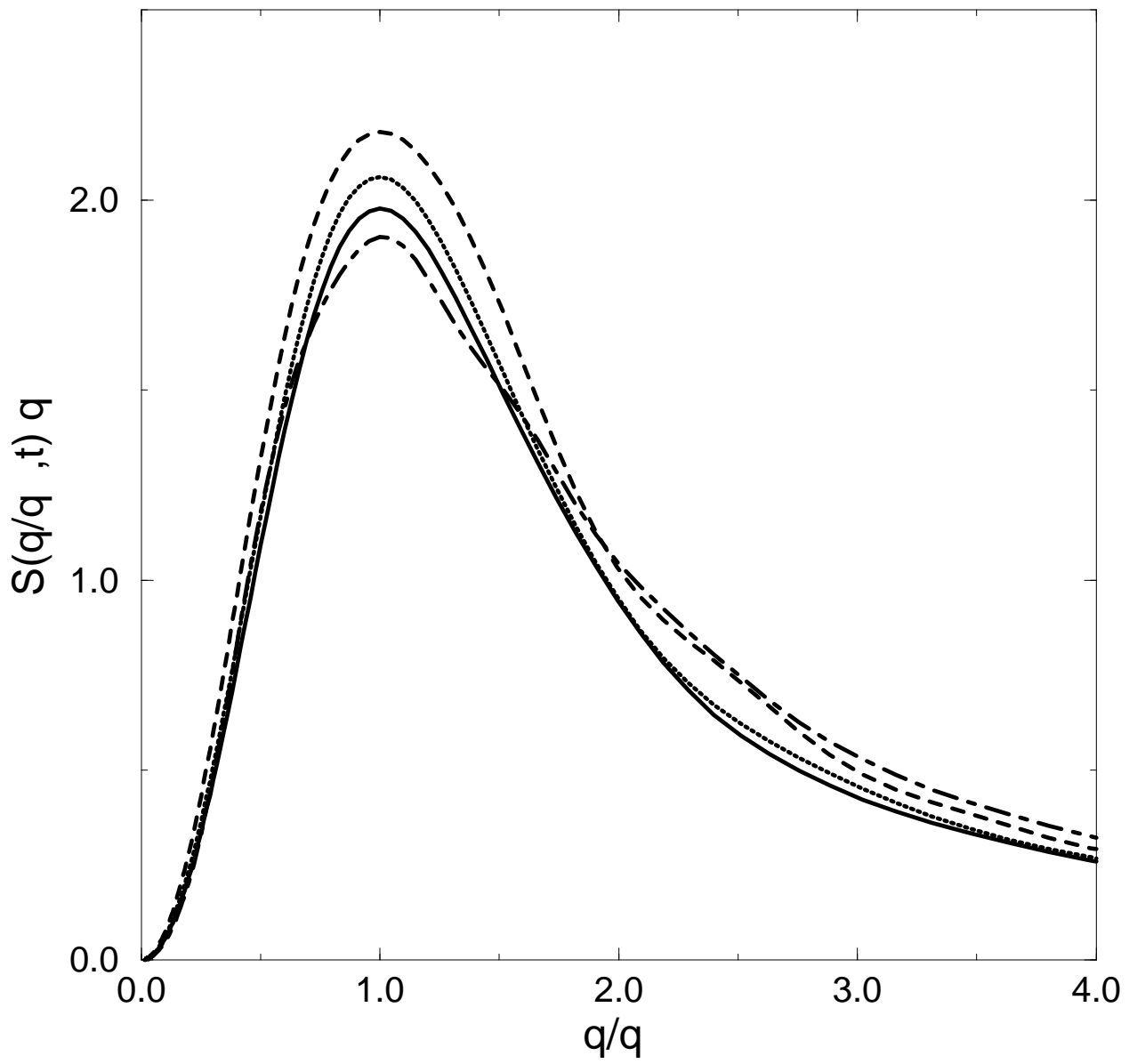


fig 7

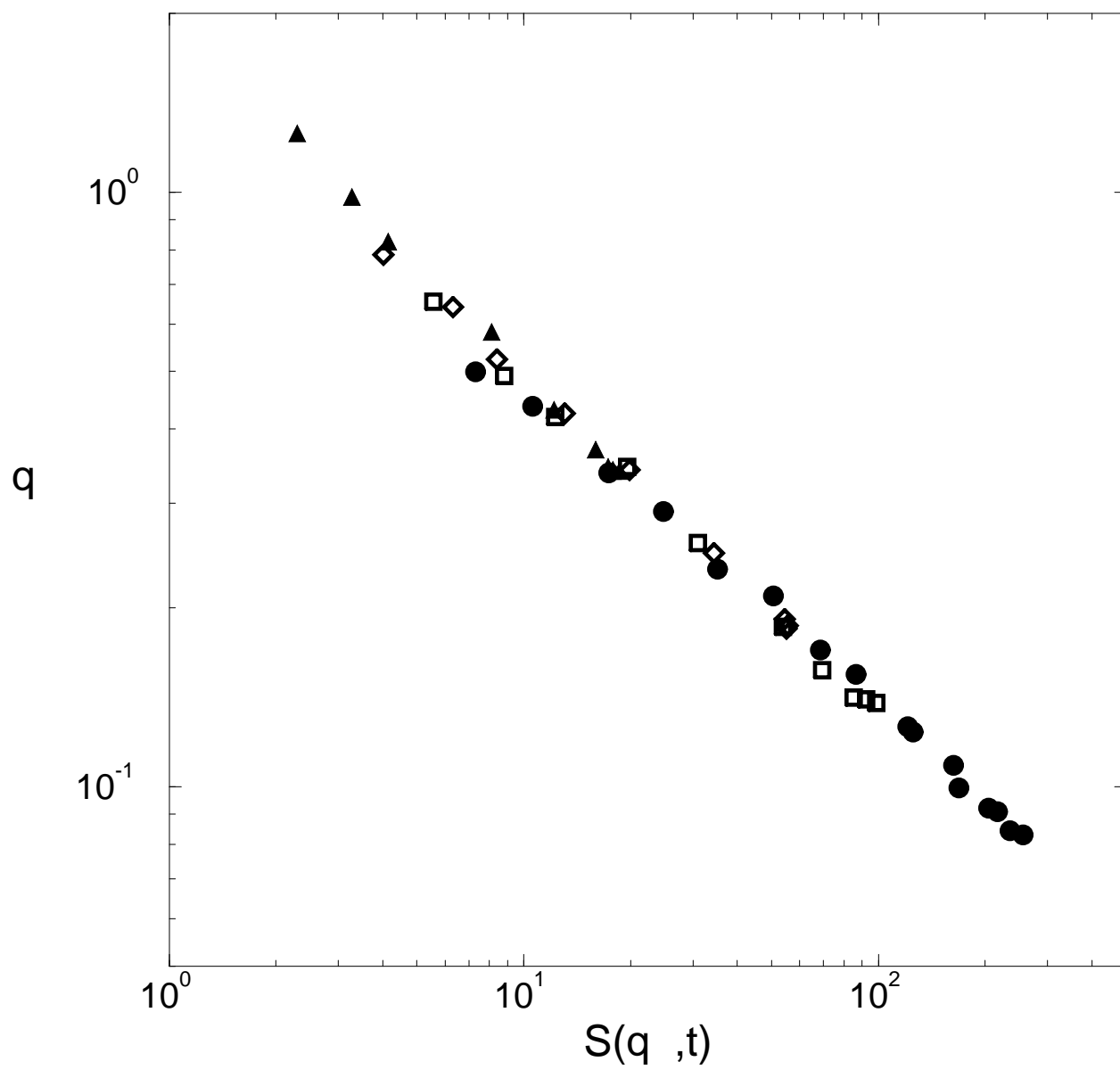


fig 8

